CENTRE DE RECERCA MATEMÀTICA

Preprint núm. 1185
February 2014

Mathematical model for the melting of nanoparticles with a density jump

F. Font, T.G. Myers, S.L. Mitchell

MATHEMATICAL MODEL FOR THE MELTING OF NANOPARTICLES WITH A DENSITY JUMP

F. FONT, T. G. MYERS, AND S.L. MITCHELL

Abstract. The melting process of spherical nanoparticles is analyzed in this paper using a mathematical model based in continuum theory. For the first time the density change between phases is taken into account in a model describing the melting of nanoparticles. This alters the standard governing equations and the effect is clearly reflected in the results. The system consists of heat equations in the solid and the liquid, and a Stefan condition providing an equation for the evolution of the melt boundary. The Gibbs-Thomson effect describing the depression of the melting temperature is included in the model as a boundary condition. Approximate analytical solutions and numerical simulations are provided. The frequent assumption of equal densities in models of this kind is found to be very inaccurate when compared to the general solution for particles with radii ranging from 10 to 100 nm. Phase change and Nanoparticle and Expansion and Melting

1. Introduction

There is a large body of work concerning the mathematical modelling of phase change. The original Stefan problem concerned the formation of sea ice. Since then the model has been applied to many different forms of phase change and geometries as well as topics in porous media flow and finance [1]. An analogous problem occurs in growth of material from a saturated liquid, where concentration rather than temperature gradients drive the growth [2]. In the context of phase change the vast majority of studies incorporate a number of restrictive assumptions, which are often made for mathematical convenience and limit the applicability of the results to highly idealised situations. Alexiades and Solomon [3, Chap. 1] provide a list of standard assumptions including constant latent heat, constant phase change temperature, a sharp phase change interface, constant thermal properties in each phase and a constant density which is equal in both phases. They state that this final assumption is perhaps the most unreasonable, indeed anyone with experience of burst water pipes will be aware of the true importance of density change. Consequently, in this paper we will focus on the effect of density change. Our work is motivated by the melting of spherical nanoparticles however the model could be applied to more general situations of practical interest, such as pipe bursting, cryopreservation, phase change microvalves and metal casting, see [3, 4, 5, 6, 7].

CRM Preprint Series number 1185

[3] discuss freezing and melting with the incorporation of a density change. They state that most physical properties vary to some extent with temperature, but that at the phase change temperature there is often a sudden change. Although the value of the density may not change as much as other variables, its variation may lead to the most pronounced effects. They subsequently analyse phase change in Cartesian co-ordinates to show that the density jump introduces a non-standard term, proportional to the cube of the phase change velocity, into the Stefan condition. They discuss how neglecting this term can lead to over or under estimation of the front velocity depending on the physical situation. However, they later neglect this term to permit exact similarity solutions. [7] take a similar approach, again to find similarity solutions. [8] neglect the cubic term altogether and seek small time and similarity solutions for the freezing of a liquid layer and phase change in a porous half-space. In the following work we will demonstrate the importance of the cubic term, particularly near the beginning and end of the process.

At the nano-scale an important effect is that of melting point depression, which can lead to rapid melting as the particle size tends to zero. This may explain the sudden disappearance of particles discussed in [9]. The variation of the melt temperature with size is often represented by the Gibbs-Thomson equation, although there exist a number of other forms with the common feature that the temperature change is proportional to curvature [10, 9, 11, 12]. In the following work we will employ the classical Gibbs-Thomson relation

$$T_m = T_m^* \left(1 - \frac{2\sigma_{sl}\kappa}{\rho_s L_f}\right) \tag{1}$$

where T_m^* is the bulk melting temperature, σ_{sl} the surface energy between the solid and the liquid, L_f the latent heat and ρ_s the density. The curvature for spheres is $\kappa = 1/R$, where R is the particle radius. [13] look for small time and large Stefan number solutions to a two-phase problem describing the melting of spherical nanoparticles subject to (1). [14] focus on the situation where the specific heats vary through the phase change. To account for this they apply a more general form of the Gibbs-Thomson relation. Their results show that melting point depression is extremely important in predicting the melt time of nanoparticles. They also investigate the effect of using the generalised Gibbs-Thomson as opposed to the above classical version. [15] had previously concluded that melting point depression could explain the rapid melting of nanoparticles. To simplify the mathematics their work used an approximation where the variation of specific heat was neglected in the Gibbs-Thomson relation but retained in the remaining governing equations. In [14] it was shown that, when compared to using the generalised Gibbs-Thomson relation, this approach leads to differences on the order of 10% in melt times for 10 nm particles, whilst for 100 nm particles the difference is around 1%. In the following study we will see that allowing the density to vary can more than double the melt time of a 10 nm particle. Thus,

CRM Preprint Series number 1185

in order to keep the analysis simple and focus on the density variation, we will assume the specific heats to be equal for both phases and model the melting point depression with (1).

The mathematical model to be developed in the following section will be based on continuum theory. Since our focus is on nanoscale phase change it is worth considering the validity of this theory. This issue is discussed in detail in [14]. To summarise, they state that comparison of molecular dynamics simulations, experiment and continuum theory have led to the conclusion that for fluid flow continuum theory may be accurate down to around 3 nm, for heat transfer and phase change 2 nm appears to be the lower limit, see [16, 17]. Consequently, we do not expect our model to be valid below this value.

In section 2 of this paper we set a mathematical model that appropriately describes the melting of spherical nanoparticles. The model includes the characteristic melting point depression of nanoparticles and the effect of density change between phases. In section 3 we seek asymptotic solutions for large Stefan number by means of the perturbation method. Then, we pinpoint the small time behaviour of the system and use it later on to initialize the numerical scheme described in section 4. Results are presented in section 5, comparing the numerical and approximate solutions. Finally, in section 6 we highlight the main conclusions of this study.

2. Mathematical model

We consider a solid sphere with radius R_0, initially at the melting temperature $T_m(R_0)$, given by the Gibbs-Thomson equation (1). The surface of the sphere is suddenly raised to $T_H > T_m(R_0)$ which starts the melting process: a liquid phase grows from the surface of the particle inwards until the whole solid disappears. We denote the moving solid-liquid interface by $R(t)$. The liquid phase moves due to the density change between phases. Therefore, the outer surface of the sphere also moves, and it is designated as $R_b(t)$, where $R_b(0) = R_b(0)$. A sketch of the model is presented in figure 1.

To describe the melting process of the nanoparticle requires solving heat equations in the solid and liquid phases over the moving domains $0 < r < R(t)$ and $R(t) < r < R_b(t)$, respectively. The heat equation in the liquid is given by

$$\rho_l c_l \left(\frac{\partial T}{\partial t} + \nabla T \cdot \mathbf{v} \right) = k_l \nabla^2 T \,, \tag{2}$$

where T is the temperature, $\mathbf{v}$ is the velocity of the fluid, k_l the thermal conductivity and c_l the specific heat. Since the geometry is spherical and the temperature applied on the surface $R_b(t)$ is constant we may assume spherical symmetry. The velocity may be written as $\mathbf{v} = (v(r), 0, 0)$ and the heat equation becomes

$$\rho_l c_l \left(\frac{\partial T}{\partial t} + v \frac{\partial T}{\partial r} \right) = k_l \frac{1}{r^2} \frac{\partial}{\partial r} \left(r^2 \frac{\partial T}{\partial r} \right) \qquad \text{on} \qquad R(t) < r < R_b(t). \tag{3}$$

CRM Preprint Series number 1185

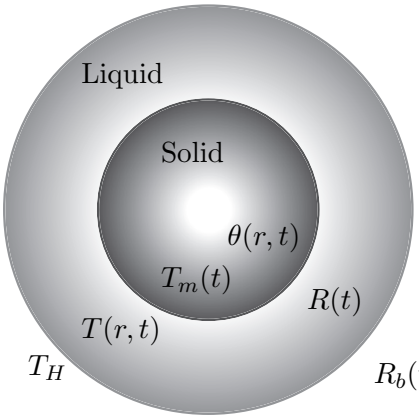

FIGURE 1. Sketch of the model, showing a solid sphere of radius $R(t)$ surrounded by a liquid layer with radius $R_b(t)$.

We find this equation widely used in the literature when dealing with phase change problems that include either shrinkage or expansion of one of the phases, see [3, 7, 18] for example.

Under the assumption of incompressible flow the velocity $\mathbf{v}$ can be determined from the continuity equation $\nabla \cdot \mathbf{v} = 0$. In the present case,

$$\frac{1}{r^2}\frac{\partial}{\partial r}\left(r^2 v\right) = 0 \tag{4}$$

leading to

$$v = \frac{h}{r^2} \tag{5}$$

where h is a constant of integration. Mass conservation requires

$$\frac{d}{dt}\left[\rho_s \frac{4}{3}\pi R^3 + \rho_l \frac{4}{3}\pi\left(R_b^3 - R^3\right)\right] = 0 \tag{6}$$

this provides an equation for the velocity of the outer surface

$$\frac{dR_b}{dt} = -\frac{R^2}{R_b^2}\left(\frac{\rho_s}{\rho_l} - 1\right)\frac{dR}{dt}. \tag{7}$$

Noting that $v(R_b) = dR_b/dt$ provides an expression for h in (5),

$$v = -\frac{R^2}{r^2}\left(\frac{\rho_s}{\rho_l} - 1\right)\frac{dR}{dt}. \tag{8}$$

The temperature in the solid phase, θ, will be given by the one dimensional heat equation

$$\rho_s c_s \frac{\partial \theta}{\partial t} = k_s \frac{1}{r^2}\frac{\partial}{\partial r}\left(r^2 \frac{\partial \theta}{\partial r}\right) \qquad \text{on} \qquad 0 < r < R(t). \tag{9}$$

CRM Preprint Series number 1185

The appropriate boundary conditions for equations (3) and (9) are

$$T(R_b,t)=T_H,\quad T(R,t)=\theta(R,t)=T_m(t),\quad \left.\frac{\partial\theta}{\partial r}\right|_{r=0}=0, \tag{10}$$

where $T_m(t)$ is given by equation (1). Energy conservation across the surface $R(t)$ gives the Stefan condition

$$\rho_s\big[L_f+(c_l-c_s)(T_m-T_m^*)\big]\frac{dR}{dt}+ \frac{\rho_s}{2}\left(1-\frac{\rho_s}{\rho_l}\right)^2\left(\frac{dR}{dt}\right)^3=k_s\left.\frac{\partial\theta}{\partial r}\right|_{r=R}-k_l\left.\frac{\partial T}{\partial r}\right|_{r=R}. \tag{11}$$

This provides a differential equation for $R(t)$ subject to the initial condition $R(0)=R_0$ (a detailed derivation of the Cartesian version with $\Delta c=0$ is given in [3]). Note, in the standard Stefan problem with a fixed temperature boundary condition $R_t\to\infty$ as $t\to 0$ (we will observe the vertical slope in the results presented later). In the idealised situation where $\rho_s=\rho_l$ the term involving R_t^3 disappears from the governing equation and the standard Stefan condition is retrieved. However, if we try to reproduce the results of this case by decreasing the factor $1-\rho_s/\rho_l$ in the above equation we do not approach the standard solution. This is because as $t\to 0$, $R_t\to\infty$ and the product $(1-\rho_s/\rho_l)R_t^3\not\to 0$. That is, we have a classic example of a singular perturbation where the results obtained by approaching a limit $(1-\rho_s/\rho_l)\to 0$ do not coincide with the actual limit $(1-\rho_s/\rho_l)=0$. In order to focus on the density difference we will now set $c_l=c_s$ and the first term in (11) subsequently reduces to $\rho_s L_f R_t$.

Finally, we assume that initially the nanoparticle is at the melting temperature, $\theta(r,0)=T_m(0)$, given by (1). Considering lower initial temperatures ($\theta(r,0)<T_m(0)$) would require solving a thermal problem previous to the melting process.

The problem may be nondimensionalized introducing the variables

$$\hat{T}=\frac{T-T_m^*}{T_H-T_m^*},\quad \hat{\theta}=\frac{\theta-T_m^*}{T_H-T_m^*},\quad \hat{r}=\frac{r}{R_0},\quad \hat{t}=\frac{k_l}{\rho_l c_l R_0^2}t. \tag{12}$$

Similarly, the nondimensional moving boundaries are $\hat{R}=R/R_0$ and $\hat{R}_b=R_b/R_0$. Dropping the hats, the governing equations (3) and (9) become

$$\frac{\partial T}{\partial t}-(\rho-1)\frac{R^2}{r^2}\frac{dR}{dt}\frac{\partial T}{\partial r}=\frac{1}{r^2}\frac{\partial}{\partial r}\left(r^2\frac{\partial T}{\partial r}\right),\qquad R<r<R_b \tag{13}$$

$$\frac{\partial\theta}{\partial t}=\frac{k}{\rho}\frac{1}{r^2}\frac{\partial}{\partial r}\left(r^2\frac{\partial\theta}{\partial r}\right),\qquad 0<r<R. \tag{14}$$

The Stefan condition is

$$\rho\beta\frac{dR}{dt}+\gamma\left(\frac{dR}{dt}\right)^3=k\left.\frac{\partial\theta}{\partial r}\right|_{r=R}-\left.\frac{\partial T}{\partial r}\right|_{r=R}, \tag{15}$$

CRM Preprint Series number 1185

TABLE 1. Approximate thermodynamical parameter values for gold. The value of σ_{sl} is taken from [10].

Substance	T_m^* (K)	L_f (J/Kg)	c_l, c_s (J/Kg·K)	ρ_l, ρ_s (kg/m^3)	k_l, k_s (W/m·K)	σ_{sl} (N/m)
Gold	1337	6.37×10^4	163/129	$1.73\times10^4/1.93\times10^4$	106/317	0.27

and the boundary conditions (10) are

$$T(R_b,t)=1, \quad T(R,t)=\theta(R,t)=-\frac{\Gamma}{R}, \quad \left.\frac{\partial\theta}{\partial r}\right|_{r=0}=0, \quad T(r,0)=-\Gamma. \tag{16}$$

The dimensionless parameters are defined by

$$\rho=\frac{\rho_s}{\rho_l}, \quad k=\frac{k_s}{k_l}, \quad \beta=\frac{L_f}{c_l\Delta T}, \quad \Gamma=\frac{2\sigma_{sl}T_m^*}{R_0\rho_s L_f\Delta T}, \quad \gamma=\frac{\alpha_l^3\rho_s}{2R_0^2k_l\Delta T}\left(\rho-1\right)^2 \tag{17}$$

where $\Delta T = T_H - T_m^*$ and $\alpha_l = k_l/\rho_l c_l$ is the thermal diffusivity. Note that R_b and R are related by $R_b^3 = \rho - (\rho-1)\,R^3$, obtained by integrating the expression (7).

An extra parameter $c = c_s/c_l$ describing the difference in specific heats between phases often appears in the literature. In the present study we assume $c = 1$ (see from table 1 that $c = 0.79$, for gold). By doing this we can make use of the classical Gibbs-Thomson equation (1) instead of the extended nonlinear version form given in [14]. In addition, the term $\rho(1-c)T_mR_t$ would have to be included in left hand side of (15). Thus, as letting $c \neq 1$ would only increase the mathematical complexity of the model and would not contribute with relevant information to the results, we consider the assumption $c = 1$ valid for our purposes. The effect of assuming $c \neq 1$ versus $c = 1$ concerning the melting of nanoparticles is studied in detail in [14].

The present model differs from previous models concerning the melting of nanoparticles by the fact that includes the density variation between phases ($\rho \neq 1$). This results in an advection term in the heat equation for the liquid, accounting for the temperature variation due to the bulk movement of the liquid, and in a cubic term of the melt front velocity in the Stefan condition. If we constrain the densities to be equal by setting $\rho = 1$ (so $\gamma = 0$), both terms vanish and the standard form of the two-phase Stefan problem is retrieved. As we will see, this standard reduction significantly overestimates the speed of the melting process.

The parameter γ gives an idea of how relevant will be the cubic term for the solution. As $\gamma \propto 1/R_0^2$, the term will gain importance as the particle radius decreases. For instance, using values from table 1, assuming a temperature variation $\Delta T = 50$ K and an initial particle radius $R_0 = 100$ nm, one obtains $\gamma = 0.13$.

But, assuming $R_0 = 10$ nm we yet see that $\gamma = 13.26$. In [3] is stated that, in general, the cubic term in the Stefan condition is expected to be ignorably small compared to the linear. In our study we show, in fact, that the term is dominant for particles below 100 nm radius, and therefore, cannot be ignored if one wishes to accurately describe the melting process of nanoparticles.

Another remarkable characteristic of the model is the variation of the melting temperature due to the large curvature of spherical nanoparticles. The parameter that describes the importance of this phenomena is Γ. For gold, if $\Delta T = 50$ K and $R_0 = 10$ nm then $\Gamma = 1.17$, if $R_0 = 50$ nm then $\Gamma = 0.12$. As the radius increases above 100 nm, Γ quickly decreases and the curvature effect becomes negligible.

The parameter β, known as Stefan number, is frequently used in the literature to generate approximate solutions to Stefan problems in the form of series expansions. For instance, for increases in the temperature ranging from $\Delta T = 10$ K to $\Delta T = 100$ K we will have values from $\beta = 40$ to $\beta = 4$, respectively. Working in a large Stefan number regime is a sensible assumption. Note that, due to the small volume of nanoparticles, any small increase above the melting temperature, ΔT, at the surface of the particle will be enough to almost instantaneous melt it. This permits us to find perturbation solutions making use of β^{-1} as the small perturbation parameter, as will be shown in the next section.

Finally, the parameter k does not play an important role in our analysis. Nevertheless, if one wishes to reduce the two-phase model with variable phase change temperature to a one-phase model (keeping one of the phases at the phase change temperature and studying the evolution of the other phase) [14, 19] the parameter k is crucial in order to derive appropriate energy conserving forms of the Stefan condition [20].

3. Perturbation solution

The system (13)-(15) presents the global structure of a two-phase Stefan problem: a heat equation for the liquid phase (13), a heat equation for the solid phase (14) and an equation for the position of the solid-liquid interface (15), all subject to appropriate boundary conditions (16).

To analyze the problem we make use of a standard perturbation technique. As in [14], we consider β to be large for our system (for gold heated 10 K above the bulk melt temperature $\beta \approx 40$) and define a new time scale $t = \beta\tau$. This permits us to assume expansions for the temperatures $\theta = \theta_0 + \theta_1/\beta + \mathcal{O}(1/\beta^2)$ and $T = T_0 + T_1/\beta + \mathcal{O}(1/\beta^2)$. Then, equations (13) and (14) can be expressed as a sequence of problems. The leading order problem is represented by the equations

$$0 = \frac{1}{r^2}\frac{\partial}{\partial r}\left(r^2\frac{\partial T_0}{\partial r}\right), \qquad 0 = \frac{1}{r^2}\frac{\partial}{\partial r}\left(r^2\frac{\partial \theta_0}{\partial r}\right) \tag{18}$$

CRM Preprint Series number 1185

with boundary conditions $T_0(R_b,\tau)=1$, $T_0(R,\tau)=\theta_0(R,\tau)=-\Gamma/R$, and $\theta_{0r}(0,\tau)=0$. The subsequent solutions are

$$\theta_0=-\frac{\Gamma}{R},\qquad T_0=-\frac{\Gamma}{R}+\frac{R_b}{R}\frac{(r-R)}{r}\left(\frac{R+\Gamma}{R_b-R}\right). \tag{19}$$

The $\mathcal{O}(1/\beta)$ problem has equations

$$\frac{\partial T_0}{\partial\tau}-(\rho-1)\frac{R^2}{r^2}\frac{dR}{d\tau}\frac{\partial T_0}{\partial r}=\frac{1}{r^2}\frac{\partial}{\partial r}\left(r^2\frac{\partial T_1}{\partial r}\right) \tag{20}$$

$$\frac{\partial\theta_0}{\partial\tau}=\frac{k}{\rho}\frac{1}{r^2}\frac{\partial}{\partial r}\left(r^2\frac{\partial\theta_1}{\partial r}\right) \tag{21}$$

with boundary conditions $T_1(R_b,\tau)=T_1(R,\tau)=\theta_1(R,\tau)=\theta_{1r}(0,\tau)=0$. The solutions become

$$T_1=\frac{(\Gamma+R_b)(R_b-r)(r-R)}{6(R_b-R)^2r}\left\{\frac{3(\rho-1)R(\Gamma+R)(R_b-R)}{(\Gamma+R_b)r}\right. \tag{22}$$

$$\left.+\frac{(\rho-1)R(\Gamma+R)[3-R(R_b+r+R)]}{R_b^2(\Gamma+R_b)}-r+2R_b-R\right\}R_\tau, \tag{23}$$

$$\theta_1=-\frac{\rho}{6k}\frac{\Gamma}{R^2}(R^2-r^2)R_\tau. \tag{24}$$

Now, substituting $\theta\approx\theta_0+\theta_1/\beta$ and $T\approx T_0+T_1/\beta$ into (15) within the new time scale, we obtain the following equation for the melting front

$$\frac{\gamma}{\beta^3}\left(\frac{dR}{d\tau}\right)^3+\left\{\rho-\frac{\rho\Gamma}{\beta 3R}+\frac{(R+\Gamma)}{\beta 6R}\left[\frac{(\rho-1)(3R_b-R^2R_b-2R^3)}{(R_b-R)}\right.\right. \tag{25}$$
$$\left.\left.+\frac{2(\Gamma+R_b)}{(\Gamma+R)}\right]\right\}\frac{dR}{d\tau}+\frac{R_b}{R^2}\frac{(R+\Gamma)}{(R_b-R)}=0$$

subject to the initial condition $R(0)=1$. To solve equation (25) we first set $z=dR/d\tau$ so that it can be expressed as a cubic polynomial of the form $z^3+k_1z+k_2=0$, which has one real root, say $z_1=f(R)$. Finally, $dR/d\tau=z_1$ is solved numerically. So, the original problem specified by two partial differential equations and a first order ordinary differential equation has been reduced to a cubic first order ordinary differential equation.

To obtain the solution of the model when the density jump is not taken into account, it is enough to set $\rho=1$ in (25). Note, by doing this we are also saying that $\gamma=0$ and $R_b=1$. Then, (25) becomes

$$\left(1+\frac{1}{3\beta R}\right)\frac{dR}{d\tau}+\frac{\Gamma+R}{R^2(1-R)}=0,\qquad R(0)=1 \tag{26}$$

with solution

$$-\beta(1-R^3)+a(1-R^2)-b(1-R)+b\Gamma\ln\left(\frac{\Gamma+1}{\Gamma+R}\right)=3\beta\tau \tag{27}$$

where $a=[3\beta(\Gamma+1)-1]/2$ and $b=(\Gamma+1)(3\beta\Gamma-1)$. In section 5 we will compare the solutions of (25) with (27) for different parameter values and see how the melting times are affected by neglecting the density jump between phases.

Initial conditions are often an issue when solving Stefan problems [21]. Therefore, it is convenient to analyze the behavior of $R(t)$ for small times. This can be done by studying the limit $t\to 0$ in the Stefan condition (15). We rescale the space variable r as $\eta=(r-R)/(R_b-R)$ on $R<r<R_b$ and as $\xi=r/R$ on $0<r<R$, transforming (15) into

$$(R_b-R)\left[\rho\beta\left(\frac{dR}{dt}\right)+\gamma\left(\frac{dR}{dt}\right)^3\right]=k\frac{(R_b-R)}{R}\left.\frac{\partial\theta}{\partial\xi}\right|_{\xi=1}-\left.\frac{\partial T}{\partial\eta}\right|_{\eta=0} \tag{28}$$

As we are interested in the limit $t\to 0$ we rescale time as $t=\epsilon\hat{\tau}$, where $\epsilon\ll 1$. Then, as we want to satisfy the initial condition, $R(0)=1$, we propose $R(t)$ to be of the form

$$R=1-\lambda(\epsilon\hat{\tau})^p, \tag{29}$$

where p, λ are constant and $p<1$. By substituting (29) in (28) we obtain

$$-\lambda(\epsilon\hat{\tau})^p\left[\rho\beta\lambda p(\epsilon\hat{\tau})^{p-1}+\gamma(\lambda p)^3(\epsilon\hat{\tau})^{3p-3}\right]=k\lambda(\epsilon\hat{\tau})^p\left.\frac{\partial\theta}{\partial\xi}\right|_{\xi=1}-\left.\frac{\partial T}{\partial\eta}\right|_{\eta=0} \tag{30}$$

where we have used the definition of R_b to show $(R_b-R)\to\lambda(\epsilon\hat{\tau})^p$ as $t\to 0$. In (30) there are a number of possibilities for the leading order balance. The melting is driven by the temperature gradient in the liquid T_r so we expect this to cause one of the terms $(\epsilon\tau)^{2p-1}$ or $(\epsilon\tau)^{4p-3}$ indicating $p=1/2$ or $p=3/4$. When $\gamma\neq 0$ ($\rho\neq 1$) the largest term has $p=3/4$, when $\gamma=0$ then the power must be $p=1/2$ for equation (30) to balance. Hence for small times we will have

$$R\approx\begin{cases}1-\lambda_1 t^{3/4} & \text{if } \gamma\neq 0\\ 1-\lambda_2 t^{1/2} & \text{if } \gamma=0.\end{cases} \tag{31}$$

In the next section we will determine λ_1, λ_2. Note, as discussed earlier both of these solutions indicate $R_t\to\infty$ as $t\to 0$.

4. Numerical solution method

The approximate solutions found for T, θ and R, are compared with the numerical solution of (13)-(16) by finite differences. The equations (13)-(14) are transformed by applying the change $v=r\theta$ and $u=rT$. This converts (14) into a planar heat equation and (13) in somewhat more complicated but easy to switch from $\rho\neq 1$ to $\rho=1$ when comparing the two cases. Then, the variables $\eta=(r-R)/(R_b-R)$ and $\xi=r/R$ employed in (28) are used to immobilize

the boundaries of u and v, respectively. Hence, we are left with the following governing equations

$$\frac{\partial v}{\partial t} = \frac{R_t}{R}\xi\frac{\partial v}{\partial \xi} + k\frac{1}{R^2}\frac{\partial^2 v}{\partial \xi^2} \qquad \text{on} \qquad 0 < \xi < 1 \tag{32}$$

and

$$\begin{aligned}(R_b - R)^2\frac{\partial u}{\partial t} =& \frac{\partial^2 u}{\partial \eta^2} - \frac{(\rho-1)(R_b-R)^2R^2}{[R+\eta(R_b-R)]^3}R_t u \\ &+ (R_b - R)\left\{\left[1 + \frac{(\rho-1)R^2}{[R+\eta(R_b-R)]^2} - \eta\right]R_t + \eta R_{bt}\right\}\frac{\partial u}{\partial \eta}\end{aligned} \tag{33}$$

on $0 < \eta < 1$. The Stefan condition becomes

$$\rho\beta R^2\frac{dR}{dt} + \gamma R^2\left(\frac{dR}{dt}\right)^3 = k\frac{\partial v}{\partial \xi}\bigg|_{\xi=1} - \frac{R}{(R_b-R)}\frac{\partial u}{\partial \eta}\bigg|_{\eta=0} + (k-1)\Gamma \tag{34}$$

where $R(0) = 1$, and the boundary conditions for the temperatures are $v(0,t) = 0$, $v(1,t) = u(0,t) = -\Gamma$ and $u(1,t) = 1$. Then, a semi-implicit scheme is employed, discretizing implicitly for u, v and explicitly for R, R_t in (32)-(33). The discrete forms of the partial derivatives are

$$\frac{\partial v}{\partial t} = \frac{v_i^{n+1} - v_i^n}{\Delta t}, \qquad \frac{\partial v}{\partial \xi} = \frac{v_{i+1}^{n+1} - v_{i-1}^{n+1}}{2\Delta\xi}, \qquad \frac{\partial^2 v}{\partial \xi^2} = \frac{v_{i+1}^{n+1} - 2v_i^{n+1} + v_{i-1}^{n+1}}{\Delta\xi^2} \tag{35}$$

where $i = 1, \ldots, I$ and $n = 1, \ldots, N$, and analogously for u. By means of (35) equations (32)-(33) can be expressed as a matrix system and are solved at each time step n. The position of the melting front is obtained from (34) using the time derivative

$$\frac{dR}{dt} = \frac{R^{n+1} - R^n}{\Delta t} \tag{36}$$

and a three point backward difference for the partial derivatives.

The liquid phase does not exist at $t = 0$. Note, there is a jump in the temperature introduced by the boundary conditions $u(0,t) = -\Gamma$ and $u(1,t) = 1$ as $t \to 0$. In order to avoid this discontinuity and initialize the numerical scheme, consistent initial conditions have to be found. This can be achieved by substituting (31) in (33) and (34), and studying the limit $t \to 0$. In the case where $\gamma \neq 0$ the limiting case gives the problem

$$\frac{d^2u}{d\eta^2} = 0, \quad u(0) = -\Gamma, \quad u(1) = 1, \quad \left(\frac{3}{4}\right)^3\lambda_1^4\rho = \frac{\partial u}{\partial \eta}\bigg|_{\eta=0} \tag{37}$$

which leads to

$$u = (\Gamma+1)\eta - \Gamma, \qquad \lambda_1 = \left(\frac{4}{3}\right)^{3/4}\left(\frac{\Gamma+1}{\rho}\right)^{1/4}. \tag{38}$$

CRM Preprint Series number 1185

For the case $\gamma = 0$ we obtain

$$\frac{d^2u}{d\eta^2} - \frac{\lambda_2^2}{2}(1-\eta)\frac{du}{d\eta} = 0, \quad u(0) = -\Gamma, \quad u(1) = 1, \quad \beta\frac{\lambda_2^2}{2} = \left.\frac{du}{d\eta}\right|_{\eta=0} \tag{39}$$

leading to

$$u = 1 - (1+\Gamma)\frac{\operatorname{erf}(\lambda_2(1-\eta)/2)}{\operatorname{erf}(\lambda_2/2)} \tag{40}$$

where λ_2 is the solution of the transcendental equation

$$\frac{1}{2}\sqrt{\pi}\,\beta\,\lambda_2\,e^{\lambda_2^2/4}\,\operatorname{erf}\,(\lambda_2/2) = 1+\Gamma. \tag{41}$$

Expressions (38) and (40)-(41) are used as initial conditions to start the codes.

5. Results and discussion

In this section we present a set of results for the melting of a spherical nanoparticle. We use data appropriate for gold (as shown in Table 1) since this is a very common material for nanoparticles. The density change between solid and liquid gold is within the range of many materials, so it provides typical results.

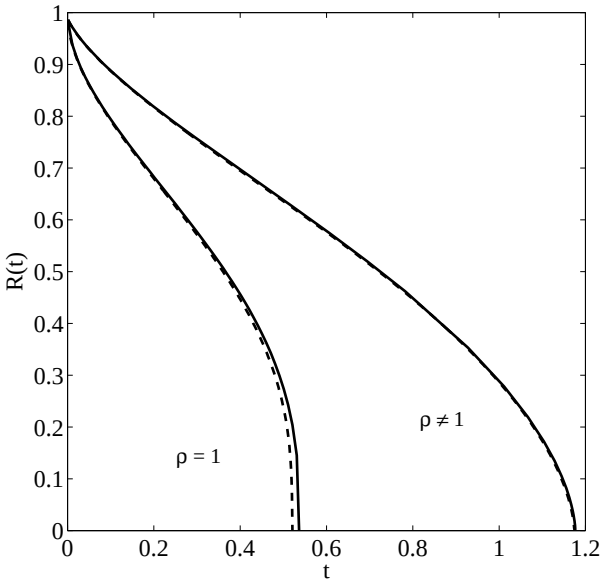

Figure 2. Evolution of the nondimensional melting front $R(t)$ for the two cases of study $\rho=1$ and $\rho\neq 1$, for $\beta=100$ and $R_0=10$ nm.

In Figure 2 we plot the evolution of the solid-liquid interface, $R(t)$, for a nanoparticle with initial dimensional radius 10 nm and $\beta = 10$ (which corresponds to relatively slow melting). Two pairs of curves are shown, one for the

case $\rho = 1$, the other for $\rho \approx 1.116$. The solid lines represent the solution of the equations derived from the perturbation analysis, i.e. the solution for $\rho = 1$ given by (27), the other for $\rho \neq 1$ given by (25), the dashed line is the numerical solution. In both cases the perturbation solution is very close to the numerical solution, indicating a full numerical analysis is not necessary. It is quite clear that the two sets of solutions lead to very different melt times. When $\rho = 1$ the melt process takes approximately half the time of that obtained with the correct change in density, $\rho \approx 1.116$. Both sets of curves show a melt velocity $R_t \to -\infty$ at the final stages of melting. We associate this with the sudden melting of nanoparticles as $R \to 0$, observed experimentally in [9] and already discussed and analyzed in previous theoretical studies [13, 14].

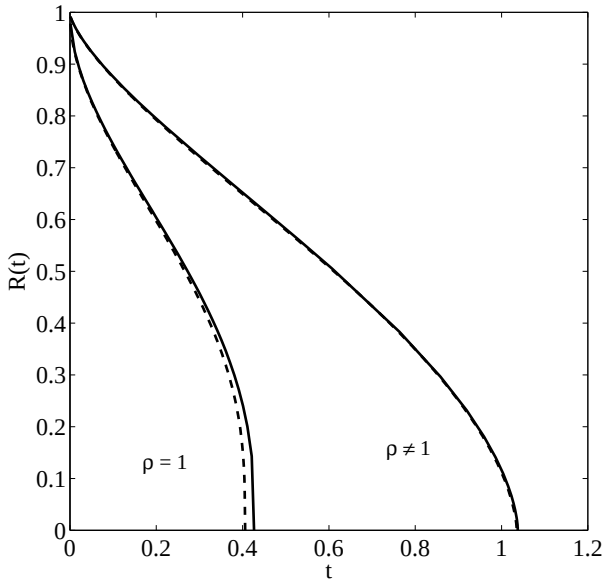

FIGURE 3. Evolution of the nondimensional melting front $R(t)$ for the two cases of study $\rho = 1$ and $\rho \neq 1$, for $\beta = 10$ and $R_0 = 10$ nm.

In Figure 3 we present two sets of results for the same initial radius, but now $\beta = 10$. Since $\beta \propto 1/\Delta T$ we expect faster melting than in the previous example and this is obviously the case. However, the results are qualitatively similar to the $\beta = 100$ example and specifically there is a factor of greater than two difference in melt times for the two density cases. The perturbation solution, which is based on an expansion in the small parameter $1/\beta$ still shows excellent agreement with the numerical solution.

In Tables 2 and 3 we present dimensional melting times for particle radii 10, 50, 100 nm and $\beta = 5, 10, 100$ for $\rho = 1$ and $\rho \neq 1$ respectively. The dimensional times are obtained by multiplying the nondimensional melting time by the time

scale $\rho_l c_l R_0^2/k_l$. By comparing the two tables we see that for a particle with $R_0 = 10$ nm, the computed melting times for the case $\rho = 1$ are between 56% (for $\beta = 100$) and 65% (for $\beta = 5$) faster than for the ones corresponding to $\rho \neq 1$. In the second column ($R_0 = 50$ nm), the melting times for the case $\rho = 1$ are between the 16% and 23% faster than those for $\rho \neq 1$. Finally, the third column ($R_0 = 100$ nm) present differences between the two cases of 15% and the 16%. Results for larger particles show that the difference settles at approximately 15%. This difference in melt times carries through to the macro-scale, indicating the importance of incorporating density variation within more standard Stefan problems.

TABLE 2. Melting times for the case $\rho = 1$. Results for gold.

	Melting times (s)		
	$R_0 = 10$ nm	$R_0 = 50$ nm	$R_0 = 100$ nm
$\beta = 100$ ($T_H \approx 1341$ K)	$1.38{\cdot}10^{-12}$	$1.55{\cdot}10^{-10}$	$1.07{\cdot}10^{-9}$
$\beta = 10$ ($T_H \approx 1376$ K)	$1.08{\cdot}10^{-12}$	$0.69{\cdot}10^{-10}$	$0.34{\cdot}10^{-9}$
$\beta = 5$ ($T_H \approx 1415$ K)	$0.89{\cdot}10^{-12}$	$0.45{\cdot}10^{-10}$	$0.21{\cdot}10^{-9}$

TABLE 3. Melting times for the case $\rho \neq 1$. Results for gold.

	Melting times (s)		
	$R_0 = 10$ nm	$R_0 = 50$ nm	$R_0 = 100$ nm
$\beta = 100$ ($T_H \approx 1341$ K)	$3.12{\cdot}10^{-12}$	$1.84{\cdot}10^{-10}$	$1.26{\cdot}10^{-9}$
$\beta = 10$ ($T_H \approx 1376$ K)	$2.75{\cdot}10^{-12}$	$0.85{\cdot}10^{-10}$	$0.41{\cdot}10^{-9}$
$\beta = 5$ ($T_H \approx 1415$ K)	$2.49{\cdot}10^{-12}$	$0.58{\cdot}10^{-10}$	$0.25{\cdot}10^{-9}$

The physical mechanism behind the slower melting when $\rho \neq 1$ is easily explained by considering the energy in the system. Melting occurs due to heat being input at the boundary R_b. When $\rho = 1$ this energy goes to heating up the material and driving the phase change. However, when $\rho \neq 1$ the fluid must move due to the expansion (or contraction depending on the material) caused by the phase change. This provides another energy sink, namely kinetic energy, which then results in less energy available to melt the material. Mathematically we can see from equation (31) that when $\rho = 1$ the initial melt rate $R_t \propto t^{-1/2}$ is much greater than when $\rho \neq 1$, $R_t \propto t^{-1/4}$.

To understand why the two sets of results remain different even for large particles we may consider the Stefan condition (15). When $\rho = 1$ the second term

CRM Preprint Series number 1185

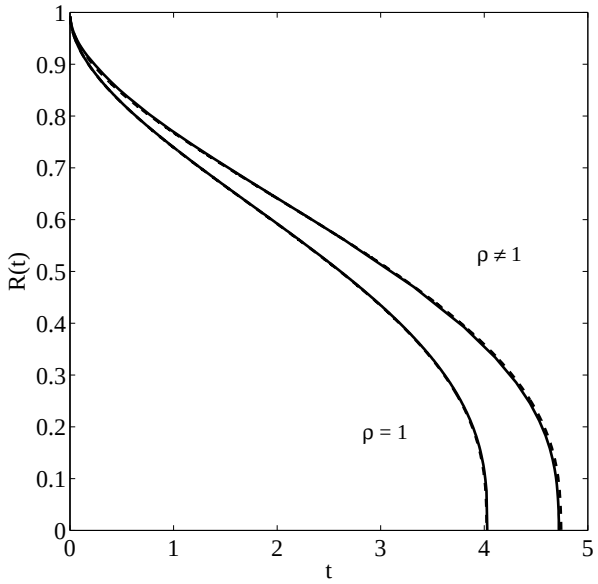

FIGURE 4. Evolution of the nondimensional melting front $R(t)$ for the two cases of study $\rho = 1$ and $\rho \neq 1$, for $\beta = 100$ and $R_0 = 100$ nm.

on the left hand side is zero (since the parameter $\gamma \propto \rho - 1 = 0$). When $\rho \neq 1$ then $\gamma \neq 0$ and the term R_t^3 plays a role. The importance of the particle size also comes through $\gamma \propto 1/R_0^2$, hence the cubic term plays a greater role as R_0 decreases (which is why Figures 2, 3, with $R_0 = 10$ nm, show much greater differences than those in Figures 4, 5 where $R_0 = 100$). But then why does the difference not disappear as $R_0 \to \infty$? The reason is that, as mentioned in §2, the model with $\gamma \to 0$ does not tend to the model with $\gamma = 0$. When $\gamma \neq 0$ the Stefan condition is cubic in R_t (and so has three roots), when $\gamma = 0$ the equation is linear in R_t and has only one root so there is a fundamental difference in models. In fact, this is a classic example of a singular perturbation [22, Chap. 1]. The problem may also be viewed in the light that as $t \to 0^+$ or $t \to t_e^-$ the melt velocity $R_t \to -\infty$, hence even though $\gamma \to 0$ it is multiplying a term that tends to infinity which in this case leads to a non-negligible contribution. In Figure 6 we demonstrate the relative strength of the two terms constituting the left hand side of equation (15) for the cases where $R_0 = 10, 100$ nm and $\beta = 10$. The dashed line shows the result for $R_0 = 10$ nm. Since its value is close to or greater than unity throughout the melt process this signifies the cubic term is generally dominant. When $R_0 = 100$ nm the cubic term is negligible for most of the process, but the peaks at the beginning and end mean that it still plays an important role there. Increasing γ further will push the position of the peaks towards the initial and final times, but will never remove

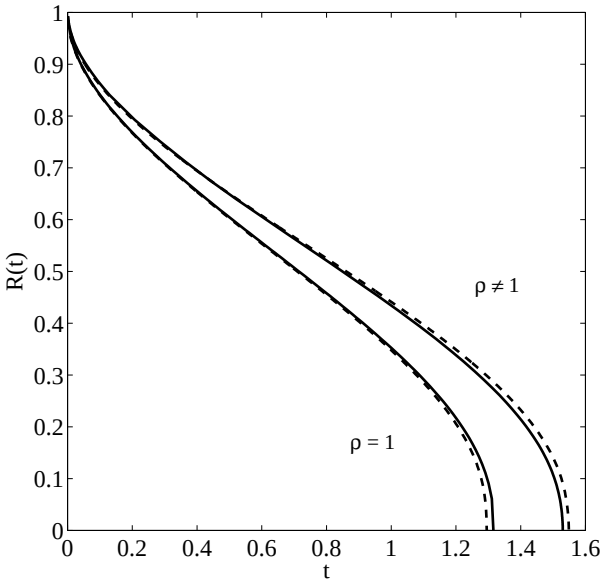

FIGURE 5. Evolution of the nondimensional melting front $R(t)$ for the two cases of study $\rho = 1$ and $\rho \neq 1$, for $\beta = 10$ and $R_0 = 100$ nm.

them. This is what leads to the 15% difference in results and means that even for macro-scale problems we should expect a significant error if the difference in densities between phases is ignored.

With no experimental results which exactly describe our theoretical models we must rely on similar studies to provide estimates and at least quantitative agreement. For instance, in [23] the melting of gold nanoparticles is studied experimentally by time resolved x-ray scattering when heated up by a laser beam. They find that the time to complete melting is less than 100 ps for nanoparticles with $R_0 = 50$ nm. In [24] the melting of 2 and 20 nm gold nanoparticles is studied, finding melting times on the picosecond scale. Our results show indeed the right order of magnitude, however we are not aware of the existence of any experimental studies that could further validate the accuracy of our results.

6. Conclusions

The main aim of this paper was to determine whether the standard modelling assumption, that the density remains constant throughout the phase change, is valid in the context of nanoparticle melting. Our results clearly showed that as the particle radius decreases the effect of the density change becomes increasingly important. We presented results for the melting of gold and found that melt times for a particle with initial radius 10 nm were more than doubled when the density ratio was changed from $\rho = 1$ to $\rho \approx 1.116$. This increase in melt time may be

CRM Preprint Series number 1185

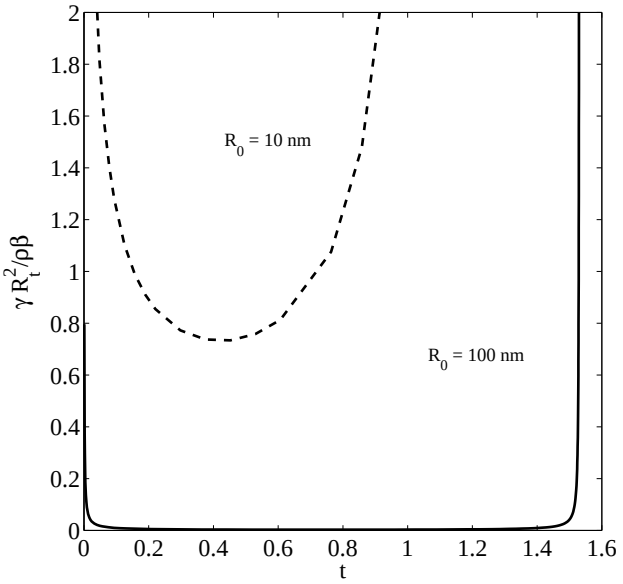

FIGURE 6. Relative importance of the term γR_t^3 against $\rho\beta R_t$ for $\beta = 10$, for nanoparticles with radius $R_0 = 100$ nm (solid line) and $R_0 = 10$ nm (dashed line).

attributed to the fact than with $\rho = 1$ the liquid phase remains stationary so all energy input into the system is converted to heat or to drive the phase change. If $\rho \neq 1$ then the liquid is forced to move which requires kinetic energy and means less energy is available for the phase change.

We therefore conclude that any mathematical model of nanoparticle melting should incorporate density variation. In fact our results show an even stronger conclusion, namely that in general the density variation should be included in phase change models. In the case studied in the present paper the difference in melt times (neglecting or including density variation) tended to a limit of approximately 15% as the particle size increased.

Acknowledgements. The research of TGM was supported by a Marie Curie International Reintegration Grant *Industrial applications of moving boundary problems* Grant no. FP7-256417 and Ministerio de Ciencia e Innovación Grant MTM2011-23789. FF acknowledges the support of a Centre de Recerca Matemàtica PhD grant. SLM acknowledges the support of the Mathematics Applications Consortium for Science and Industry (MACSI, www.macsi.ul.ie) funded by the Science Foundation Ireland Mathematics Initiative Grant 06/MI/005. The authors acknowledge Gloria Garcia for her contribution in the art work of the manuscript.

References

[1] J. Ockendon, A. Lacey, A. Movchan, and S. Howison. *Applied Partial Differential Equations*. Oxford University Press, 1999.

[2] S.H. Davis. *Theory of solidification*. Cambridge University Press, 1st edition, 2001.

[3] V. Alexiades and A.D. Solomon. *Mathematical Modelling of Freezing and Melting Processes*. Hemisphere Publishing Corporation, 1st. edition, 1993.

[4] T.G. Myers and J. Low. An approximate mathematical model for solidification of a flowing liquid in a microchannel. *Microfluid Nanofluid*, 11:417428, 2011.

[5] T.G. Myers and J. Low. Modelling the solidification of a power-law fluid flowing through a narrow pip. *Int. J. Thermal Sci.*, 70:127–131, 2013.

[6] F Font, SL Mitchell, and TG Myers. One-dimensional solidification of supercooled melts. *International Journal of Heat and Mass Transfer*, 62:411–421, 2013.

[7] M.F. Natale, E.A. Santillan Marcus, and D.A. Tarzia. Explicit solutions for one-dimensional two-phase free boundary problems with either shrinkage or expansion. *Nonlinear analysis: Real World Applications*, 11:1946–1952, 2010.

[8] Ch. Charach and I. Rubinstein. Pressure-temperature effects in planar stefan problems with density change. *Journal of Applied Physics*, 71:1128, 1992.

[9] R. Kofman, P. Cheyssac, Y. Lereah, and A. Stella. Melting of clusters approaching 0D. *The European Physical Journal D*, 9(1-4):441–444, 1999.

[10] P. Buffat and J. P. Borel. Size effect on the melting temperature of gold particles. *Physical Review A*, 13(6):2287–2297, 1976.

[11] S. L. Lai, J. Y. Guo, V. Petrova, G. Ramanath, and L. H. Allen. Size-dependent melting properties of small tin particles: Nanocalorimetric measurements. *Physical Review Letters*, 77(1):99–102, 1996.

[12] K.K. Nanda. Size dependent melting of nanoparticles. *Pramana J. Phys.*, 72(4): 617–628, 2009.

[13] S. W McCue, B. Wu, and J. M. Hill. Micro/nanoparticle melting with spherical symmetry and surface tension. *IMA J. Appl. Math*, 74:439–457, 2009.

[14] F Font and TG Myers. Spherically symmetric nanoparticle melting with a variable phase change temperature. *Journal of Nanoparticle Research*, 15(12):1–13, 2013.

[15] B. Wu, P. Tillman, S. W. McCue, and J. M. Hill. Nanoparticle melting as a Stefan moving boundary problem. *Journal of Nanoscience and Nanotechnology*, 9(2):885–888, 2009.

[16] G. Guisbiers, M. Kazan, O. Van Overschelde, M. Wautelet, and S. Pereira. Mechanical and thermal properties of metallic and semiconductive nanostructures. *J. Phys. Chem. C*, 112:4097–4103, 2008.

CRM Preprint Series number 1185

[17] K. P. Travis, B. D. Todd, and D. J. Evans. Departure from navier-stokes hydrodynamics in confined liquids. *Physical Review E*, 55(4):4288–4295, 1997.
[18] Z. Yang, M. Sen, and S. Paolucci. Solidification of a finite slab with convective cooling and shrinkage. *Applied Mathematical Modelling*, 27:733–762, 2003.
[19] B. Wu, S. W. McCue, P. Tillman, and J. M. Hill. Single phase limit for melting nanoparticles. *Applied Mathematical Modelling*, 33(5):2349–2367, 2009.
[20] T. G. Myers, S. L. Mitchell, and F. Font. Energy conservation in the one-phase supercooled Stefan problem. *Int. Commun. Heat and Mass Transf.*, 2012.
[21] S.L. Mitchell and M. Vynnycky. Finite-difference methods with increased accuracy and correct initialization for one-dimensional Stefan problems. *Applied Mathematics and Computation*, 215(4):1609–1621, 2009.
[22] E.J. Hinch. *Perturbation methods*. Cambridge University Press, 2000.
[23] A. Plech, V. Kotaidis, S. Grésillon, C. Dahmen, and G. von Plessen. Laser-induced heating and melting of gold nanoparticles studied by time-resolved x-ray scattering. *Physical Review B*, 70(19):195423, 2004.
[24] C. Ruan, Y. Murooka, R. K. Raman, and R. A. Murdick. Dynamics of size-selected gold nanoparticles studied by ultrafast electron nanocrystallography. *Nano Letters*, 7(5):1290–1296, 2007.

F. Font
Centre de Recerca Matemàtica
Campus de Bellaterra, Edifici C
08193 Bellaterra
Barcelona, Spain
and
Departament de Matemàtica Aplicada I
Universitat Politècnica de Catalunya
Barcelona, Spain
E-mail address: ffont@crm.cat

T. G. Myers
Centre de Recerca Matemàtica
Campus de Bellaterra, Edifici C
08193 Bellaterra
Barcelona, Spain
E-mail address: tmyers@crm.cat

S.L. Mitchell
MACSI
Department of Mathematics and Statistics
University of Limerick
Limerick, Ireland
E-mail address: sarah.mitchell@ul.ie

CRM Preprint Series number 1185

CRM
CENTRE DE RECERCA MATEMÀTICA
Facultat de Ciències, UAB
08193 Bellaterra
Barcelona, Spain
www.crm.cat